Design of Conformal Cooling of an Additively Printed Aluminium Die-Casting Mold Component

J. Sviželová [a,*] , L. Socha [a] , A. Mohamed [a], M. Pinta [a], K. Koza [a], T. Sellner [a], K. Gryc [a] ,
M. Dvořák [b], M. Roh [b]

[a] Environmental Research Department, Institute of Technology and Business in České Budějovice,
Okružní 517/10, 370 01 České Budějovice, Czech Republic
[b] MOTOR JIKOV Fostron a.s., Tool Shop Division, Kněžskodvorská 2277/26, 370 04 České Budějovice,
Czech Republic
* Corresponding author: E-mail address: svizelova@mail.vstecb.cz

Abstract

The paper describes the design of conformal cooling of an aluminium die-casting mold component using numerical simulations along with validation under industrial conditions. The subject of modifications was the insert. The insert comes into direct contact with the metal during the filling of the mold and solidification of the casting and determines the internal shape of the casting. The aim was to optimize the operating temperatures of the insert, reduce thermal stress in the most exposed area, achieve a more even distribution of temperatures in its volume, and maintain the casting quality. Shape modifications were made by topology optimization to reduce the volume of the insert and achieve material savings. 3D printing was chosen as the production technology due to the wider possibilities regarding the variability of the shape of the internal cooling channels. Three geometric designs of the insert were created, and numerical simulations of the temperature field of the mold were carried out in ProCAST software for each variant. Numerical simulations were validated through the temperature field of the mold detected by a thermal camera during the casting cycle. Based on the results, the final design D was selected, for which a complete numerical simulation was performed, including the filling and solidification of the castings. The results were compared with the original variant A. By adjusting the cooling, temperatures were reduced in the most temperature-exposed area of the insert. The new insert variant D showed higher temperatures in the rest of the volume, resulting from material volume reduction. However, the temperatures became even, and the temperature gradients that existed in the original insert variant A were reduced. The simulation also showed that changes in the temperature field of variant D will not negatively affect the quality of the castings. The component will be manufactured and tested in operational conditions in the next research phase.

Keywords: HPDC, Conformal cooling, Temperature field, Numerical simulation, Mold design

1. Introduction

High-Pressure Die Casting (HPDC) is a commonly used technology in the large-scale production of aluminium castings. In this process, a melt of aluminium alloy is injected under high pressure into a tool steel mould in which the casting solidifies. The casting cycle consists of several stages: mould filling, solidification of the casting, removal of the casting, and cooling of the mould. The process is very rapid. Depending on the size of the casting, the cycle time can vary from tens of seconds to minutes.

The cycle time is largely determined by the cooling of the mould, which can account for up to 80% of the cycle time [1]. The mould for die casting of aluminium alloys is a sophisticated unit containing a system of cooling and tempering channels that ensure the optimum temperature of the mould regarding the quality of the casting. The cooling channels are designed to control the solidification of the casting while keeping the mould temperature within an acceptable range. In this respect, the limitations of conventional manufacturing technologies are still encountered. For example, channels created by drilling are easy to make, but their shape does not exactly copy the shape of the casting (especially for castings with more complex shapes) because only straight holes can be made. They are also limited by the position of the cavity in the mould and the presence of other structural parts of the mould. Therefore, they usually do not provide the optimum cooling effect. This also affects the cycle time, which is governed by the hottest point of the mould cavity.

A good cooling effect is also very important in terms of the life of the mould. The mould material is stressed by thermal fatigue, eventually leading to fatigue cracking [2]. This mechanism originates from the long-term effects of temperature, stress, and strain. During the cycle, the mould surface is in contact with molten metal at high temperature. As a result, the temperature in the surface layers of the mould cavity rises while the core remains cold. Consequently, compressive stresses are applied in the surface layers of the mould cavity, causing stresses in the material. Plastic deformation may occur due to a decrease in the strength of the material at higher temperatures. At the same time, the hardness of the surface layers of the mould cavity decreases compared to the rest of the volume [3]. Cracks may start to form when plastic deformation accumulates at a certain point [2]. The situation is more serious for thin parts of the mould, which are easier to heat. Hot work tool steels show good stability of mechanical properties at operating temperatures and abrasion resistance after heat treatment and coating [4, 5], but in order to increase the life of the mould, thermal stresses should be minimised as far as possible [2, 6].

One method for achieving fast and uniform cooling is to create conformal cooling channels [7, 8]. Conformal cooling has gained popularity with the rise of the additive manufacturing of metallic materials [6, 9-13]. The wider design possibilities associated with additive manufacturing allow for more sophisticated designs for the cooling of mould inserts. The shape of the channels and surface size, the distance from the surface of the mould cavity, and the distance between channels must be considered when designing conformal cooling [1]. Numerical simulations [8, 10, 13-16] are available to optimise the design of conformal cooling, allowing the primary testing phase to be moved to a virtual space, thus saving the extra time and money usually associated with the production of test parts. The design of the conformal cooling channels from the mould cavity surface can also be chosen with respect to the shape and solidification of the casting to achieve a better cooling effect. In addition, the application of conformal cooling can affect the properties of the casting. It has been shown that the application of conformal cooling can improve the mechanical properties of the alloy [17]. The reason for this improvement is the reduction of the porosity in the castings and changes in the microstructure [12, 14]. These changes occur because of faster cooling of the material, where

large areas of porosity are dispersed by cooling the hottest spots and, at the same time, the dendritic grains are refined as the alloy solidifies [17]. This results in increased mould life, increased productivity, and reduced production scrap [3, 7, 8].

As part of the modernisation of production at MOTOR JIKOV Fostron a.s., 3D metal printing is being introduced into the production of moulds. This step opens wider possibilities for mould design, including the implementation of conformal cooling. This paper describes a design for the conformal cooling of an insert, which is part of a mould for High-Pressure Die Casting aluminium alloys. The application of conformal cooling aimed to alleviate the thermal stress on the component in the most exposed area and to achieve a more uniform temperature distribution in its volume while maintaining the quality of the production. The design changes to the component also included making it lighter in volume, which will also lead to a reduction in material consumption for production. Several designs were proposed, for which the temperature and stress fields were monitored. Numerical simulations in the ProCAST software were used for this purpose.

2. Investigation methods

Numerical simulations were performed using the ProCAST software package to verify the function of the conformal cooling design variants. ProCAST comprehensively addresses most castable alloys and casting processes, including die casting of aluminium alloys. Of course, it simulates the basic casting processes - filling, solidification and predicts the porosity in the castings. Using advanced physics and the finite element method, it also predicts complex processes during casting, monitors residual stresses and predicts deformations leading to dimensional deviations and shorter mould life [18]. For a better idea, a diagram of the different stages of the calculation for the mould and casting during the cycle is shown in Figure 1.

Temperature calculations during the filling and solidification of the castings and the prediction of porosity were controlled by the Thermal module, which allows the calculation of heat flux by solving the Fourier heat conduction equation (1), including the release of latent heat during solidification. A useful feature is also the prediction of heat transfer coefficients between the liquid in the cooling/tempering channels and the mould material. The calculation is performed locally so that the flow rate, shape of the channels and their diameters are properly accounted for [19]. This function provides more realistic results for the mould temperature field than using constant heat transfer coefficients and is very useful specifically for the design of conformal cooling of moulds or parts thereof.

$$\frac{\partial t}{\partial \tau} = a \cdot \left(\frac{\partial^2 t}{\partial x^2} + \frac{\partial^2 t}{\partial y^2} + \frac{\partial^2 t}{\partial z^2} \right) + \frac{q}{c_p \cdot \rho} \tag{1}$$

where t – temperature (K), τ – time (s), a – thermal conductivity coefficient ($m^2 \cdot s^{-1}$), x, y, z – coordinates (m), q – heat flux ($W \cdot m^{-2}$), c_p – heat capacity ($J \cdot K^{-1}$), ρ – density ($kg \cdot m^{-3}$).

The Fluid Flow module simulates mould filling based on the Navier-Stokes equations (2-4). A two-phase VOF model is

implemented in ProCAST, designed to deal with two or more phases, which are investigated as mutually impermeable continua [20-22]. As a result, it can predict the free surface motion during filling. The Navier-Stokes equations are solved in both liquid and gas phases and therefore provide a more accurate representation of the filling process. However, some simplifications have been adopted for the VOF solver. The liquid and gas phases at a given node have the same velocity, temperature, and pressure [19]. One of the functions of the Flow module is also the calculation of

Duration of the cycle

```
Dosing of the   →  Mold filling  →  Casting       →  Opening of   →  Part ejection  →  Spraying and   →  Closing of the
melt                               solidification     the die                           blowing            die
                                                                                        process
```

CASTING
Temperature field		
Velocity field	Stress + related defects	
Air entrainment	Porosity prediction	

DIE
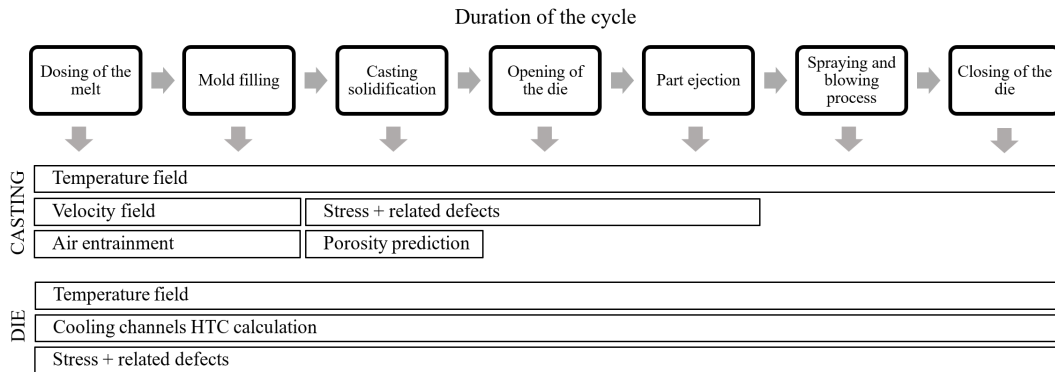| Temperature field | | |
| Cooling channels HTC calculation | | |
| Stress + related defects | | |

Fig. 1. Diagram of the different types of calculation for the mould and casting during the cycle

turbulence. In ProCAST, the two-equation turbulent RANS models (Standard k-ε model, RNG k-ε model and Realizable k-ε model) are used to calculate turbulence, which in addition to the Navier-Stokes equations, solve two transport equations for the turbulent kinetic energy k and the dissipation of the turbulent kinetic energy ε [23]. In addition, the Flow module is usually combined with the Gas model for the prediction of the air entrainment in the metal.

$$a_x - \frac{1}{\rho} \cdot \frac{\partial p}{\partial x} + \nu \cdot \left(\frac{\partial^2 v_x}{\partial x^2} + \frac{\partial^2 v_y}{\partial y^2} + \frac{\partial^2 v_z}{\partial z^2} \right) = \left(\frac{dv_x}{d\tau} \right) \quad (2)$$

$$a_y - \frac{1}{\rho} \cdot \frac{\partial p}{\partial y} + \nu \cdot \left(\frac{\partial^2 v_x}{\partial x^2} + \frac{\partial^2 v_y}{\partial y^2} + \frac{\partial^2 v_z}{\partial z^2} \right) = \left(\frac{dv_y}{d\tau} \right) \quad (3)$$

$$a_z - \frac{1}{\rho} \cdot \frac{\partial p}{\partial z} + \nu \cdot \left(\frac{\partial^2 v_x}{\partial x^2} + \frac{\partial^2 v_y}{\partial y^2} + \frac{\partial^2 v_z}{\partial z^2} \right) = \left(\frac{dv_z}{d\tau} \right) \quad (4)$$

where p – pressure (Pa), ν – kinematic viscosity ($m^2 \cdot s^{-1}$).

For the stress calculation in the Stress module, based on the desired results and available material data, three models can be selected – Linear-Elastic model, Elasto-Plastic model or the Elasto-ViscoPlastic model. For this work, the Elasto-Plastic model was used, which considers the yield stress of the material in addition to Young's modulus and Poisson's ratio [19].

Test aluminium castings were made on a Colosio PFO1000 machine [24] with a maximum locking force of 9,810 kN and a maximum injection force of 738 kN. During the casting cycle, images of the temperature distribution in the mold were taken. A FLIR E8XT thermal camera with a resolution of 320x240 pixels and a temperature range of -20 to +550 °C was used for this purpose.

3. Numerical simulations

3.1. Simulated variants

The subject of the research was an insert of a mould for die casting of aluminium alloys. The geometry of this part and its position in the mould is shown in Figure 2. It also acts as a cooling function for the liquid metal and thus affects the solidification process and the internal quality of the castings.

Using 3D printing technology enabled the implementation of conformal cooling in the insert. The motivation was to achieve a more even temperature distribution in the volume of the component and thus reduce internal stresses and extend the service life.
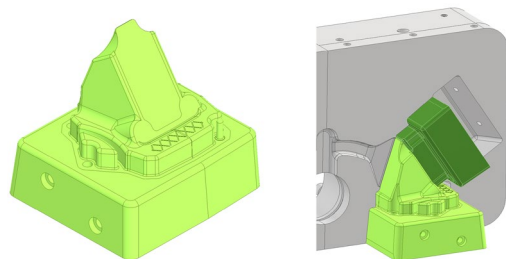

Fig. 2. Insert geometry (left) and mould fit (right)

The shape of the cooling channels was optimised to achieve more uniform temperatures in the volume of the shaped part of the insert. The conformal cooling design variants targeted the hottest area of the, which is its working part. The initial cooling for variant A was done through one large channel located in the centre of the working part of the insert (see Figure 3, variant A). In total, 3 optimised cooling circuit variants were designed, as shown in Figure 3. For variant B, a relatively dense channel network was implemented to follow the shape of the working part of the insert. Variant C tested cooling using a single spiral leading

through the insert volume to its tip. A single spiral was also applied to Variant D, taking one level of channels at the top. As the insert is made up of a relatively massive volume of metal, it was also decided during the design phase to use topological optimisation to lighten the mould. The relief of the various insert variants is shown in Figure 3. The mass parameters of the design variants are shown in Table 1. For variants B and C, the weight was reduced by up to 3.2 kg after weight reduction compared to variant A. Furthermore, variant D was designed, in which a larger volume of material was selected from the base of the insert. The weight of the insert was reduced by 7.2 kg with this modification, which represents 28% of the original weight of the insert.
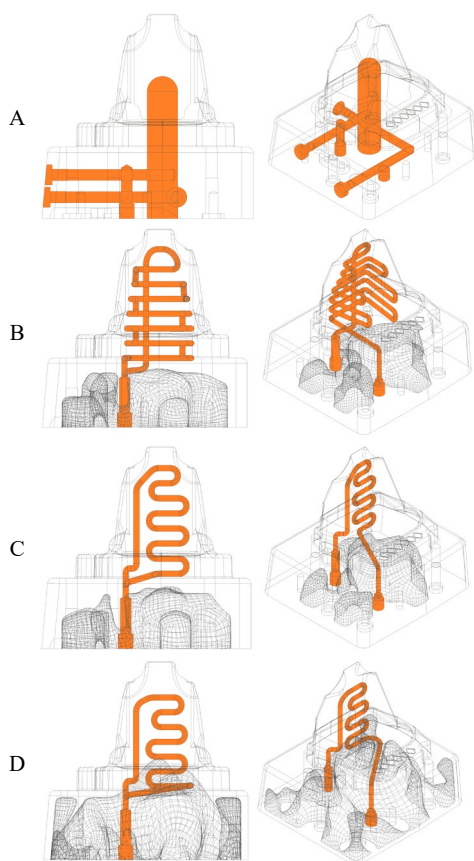

Fig. 3. Geometry of simulated insert variants

Table 1.
Weight parameters of insert variants

Variant	Weight (kg)	Weight loss compared to variant A	
		(kg)	(%)
A	25.6	-	-
B	22.4	3.2	12.5
C	22.6	3.0	11.7
D	18.4	7.2	28.1

The timing of the cooling of the insert circuit had to be adjusted depending on the changes to the design of the cooling channels. In the original variant A, the valve insert was cooled throughout the cycle time, i.e. in the interval 0 to 69 s. This setting was also used in variant B. However, there were significant drops in the temperatures of the inserts, therefore, for variants C and D, timed cooling was introduced in an interval of 13 to 21 s with an increased water flow of 5 l/min and a reduced water temperature of 20 °C. The cooling parameters for all the circuit variations are shown in Table 2. The cycling intervals are shown in Table 3.

Table 2.
Parameters of insert cooling circuits

Variant	Medium	Flow (l/min)	Temperature (°C)	Timing (s)
A	Water	3	25	0 to 69
B	Water	3	25	0 to 69
C	Water	5	20	13 to 21
D	Water	5	20	13 to 21

The numerical simulations were divided into two stages. In the first stage, a cycling calculation was performed to map the temperature field and stress states of the simulated variants. The cycling parameters, listed in Table 3, were the same for all variants. Based on the results, variant with the most suitable conformal cooling design was selected in terms of the ability to cool the insert while maintaining the quality of the casting. A complete numerical simulation was performed for this variant to map the effect of cooling on the quality of the casting. This simulation also included the filling and solidification of the casting including stress states.

Table 3.
Cycling parameters

Phase of the cycle	Start	Finish	Unit
Cycle duration	0	69	s
Mold filling	10	13	s
Casting solidification	13	21	s
Spraying	35	49	s
Blowing	49	64	s

3.2. Material properties

The insert has so far been produced from Dievar steel grade using conventional production technologies, the general chemical composition of the steel is given in Table 4. It is a chromium-molybdenum-vanadium alloyed tool steel designed for the highly demanding conditions of HPDC. It is characterised by excellent toughness and ductility in all directions, good resistance to tempering, high temperature strength, dimensional stability during heat treatment and coating and excellent hardenability [24]. The tensile properties of Dievar tool steel are shown in Figure 4. Therefore, it has been defined as the mould material for all the variants in the numerical simulations. The die castings were made at MOTOR JIKOV from EN AC-46000 alloy, whose chemical composition is shown in Table 5. This material was also used in the numerical simulations of the filling and solidification of the castings.
Table 4.

Chemical composition of Dievar tool steel (wt. %) [25]

C	Si	Mn	Cr	Mo	V
0.35	0.20	0.50	5.00	2.30	6.60

Table 5.
Chemical composition of EN AC-46000 alloy (wt. %) [26]

	Si	Fe	Cu	Mn	Mg	Cr	Ni	Zn	Pb	Sn	Ti
Min	8.0	-	2.0	-	0.05	-	-	-	-	-	-
Max	11.0	1.3	4.0	0.55	0.55	0.15	0.55	1.2	0.35	0.15	0.25
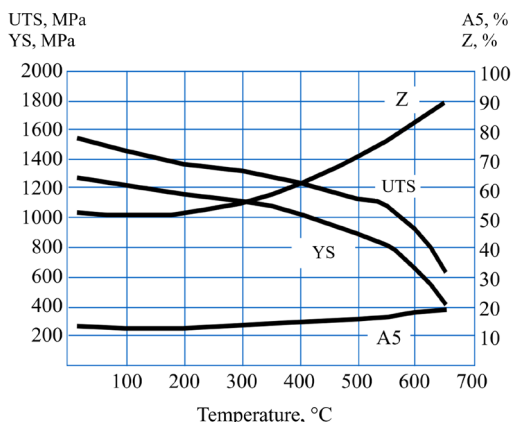
Fig. 4. Tensile properties of Dievar at elevated temperature [25]

4. Numerical model verification

Verification of the numerical simulation was made to guarantee the precision of the prediction. A thermal camera was utilised to capture images of the temperature distribution within the mold in operating conditions. Due to the limited access to the mold during the casting process, the mold was photographed approximately in the 49th s of the cycle, i.e. after the end of spraying (see Table 3). Figure 5 compares images from the thermal camera with the temperature field of the original variant A calculated by numerical simulation. The thermal camera images determined the mould temperature at specific points, as shown in Figure 5a. The temperature calculated by the numerical model was found at the analogous points. Table 6 shows a comparison of these values. In the area of the mold cavity, the deviation from the operating temperatures was approximately 2 to 7%. Temperatures at points g and h outside the mold cavity showed greater deviation. However, due to their location, points g and h were less significant in the evaluation of conformity. It can be concluded that there is a good agreement between the results of the numerical simulations and the real temperature field.
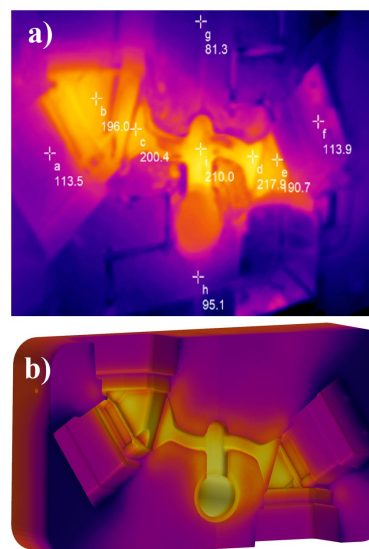

Fig. 5. Mold temperature field: a) image from a thermal camera, °C, b) temperature field calculated by numerical simulation

Table 6.
Comparison of temperatures from a thermal camera and numerical simulation

	Temperature – thermal camera (°C)	Temperature – simulation (°C)	Absolute value of the deviation (%)
a	113,5	118,7	4,4
b	196,0	200,8	2,4
c	200,4	201,6	0,6
d	217,9	203,3	7,2
e	190,7	179,2	6,4
f	113,9	111,5	2,2
g	81,3	102,1	20,4
h	95,1	111,4	14,6
i	210,0	214,0	1,9

The comparison of temperature fields confirmed that the calculation setting for variant A yielded satisfactory results. Consequently, the same settings were applied to the other simulated variants. This means only the geometry of the insert and cooling channels parameters (see Table 2) were considered.

5. Results and discussion

5.1. Temperature field

Figure 6 shows the temperature fields on the insert sections at various stages of the cycle. Figure 7 shows the temperature profiles at 3 defined points of the insert for all the simulated variants.
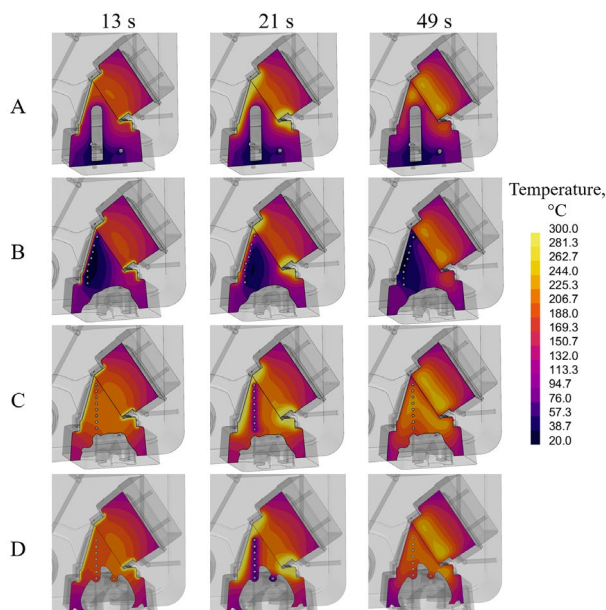
Fig. 6. Temperature fields of the variants on the insert section

Variant A represents the actual cooling design used under operating conditions. When compared to the other variants in Figure 6 and Figure 7, the cooling system of variant A was the best at removing heat from the bottom of the insert. When looking at variant B, a significant increase in the cooling intensity of the working part of the insert was evident when compared to variant A. Figure 7 shows that variant B achieved the lowest temperatures at points 1 and 3 on the working part of the insert. Compared to variant A, the temperature drop was approximately 50-70 °C, especially between the 10 and 15 second of the cycle when the mould is filled, and the casting solidifies. Under these conditions, there was a risk of overcooling the metal, which could result in surface defects. Another problem could be the location of the cooling channels, which are separated from the surface of the insert by a thin layer of material and could be subject to stresses that could lead to cracks over time. For variant C with the length of the cooling channels reduced and a shortened cooling time, temperatures increased throughout the insert volume except for the area of point 1 at the tip of the insert. The cooling effect at the tip of the insert in variant C was reflected by a decrease in temperatures in the later stages of the cycle (from about 25 s onwards), with temperatures remaining at 300-350 °C in variant A. Conformal cooling of variant C reduced these temperatures by up to 200 °C. At this stage of the cycle, mould cooling no longer influenced the quality of the casting. On the other hand, the upper level of the channels in variant C was again separated from the surface of the insert by a thin layer of material. Under these conditions, similar problems to those of variant B could again occur, so it was decided to make further modifications. This problem was solved by removing one level of the cooling channel from the tip of the insert of variant D, and the temperatures in point 1 during mould filling remained at a similar level to variant C. In the later stages of the cycle (from about 17 s onwards), the conformal cooling of variant D showed a good cooling effect at the tip of the insert even with the shortened cooling time (see

Table 2). Compared to variant A, temperatures were reduced by up to 190 °C. The temperatures in the lower non-working part of the insert were higher for the variants with conformal cooling than for variant A. This was due to the material removal during lightening. The reduced volume of the lower part of the insert heated up better. In addition, the bottom contact area of the insert downstream of the other insert components, to which some of the heat was dissipated by conduction, was reduced.

Based on these results, variant D was selected for further investigation, having a good cooling effect on the working parts of the insert even when reducing the cooling interval and reducing the risks arising from the design. At the same time, lightening was carried out for this variant, which resulted in a 28% material saving on each insert produced. Further analysis will therefore focus on the comparison of the original insert design of variant A and variant D with conformal cooling.
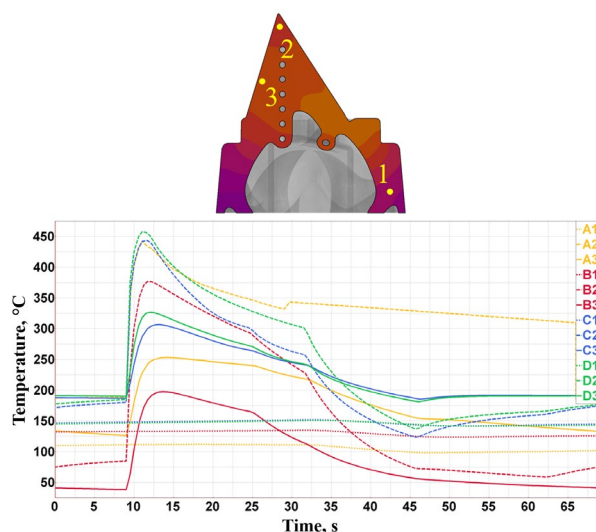

Fig. 7. Temperature profiles at selected points in the insert

5.2. Stress analysis

Figure 8 compares Principal Stress 3 in the inserts of variants A and D. This result identifies the areas where compressive stresses are applied. Figure 9 shows the compressive stress profiles of Principal Stress 3 at selected points in the regions most stressed by compressive stress. As can be seen, the compressive stresses were mainly on the working part of the insert. The working part of the insert was in contact with the liquid metal during the cycle, causing an increase in the temperature in the surface layers of the material (see Figure 6). This resulted in the development of compressive stresses, which were highest between 11 and 21 seconds in the cycle, when filling and solidification of the castings took place (see Table 3). After removing the casting, the compressive stress gradually relaxed as the insert cooled.

Figure 9 shows that the compressive stresses for variant D with conformal cooling reached higher values at points 4 and 6. This means that the variant D insert was less stressed by compressive stresses in these areas. The most significant increase

in compressive stress values occurred in the region of point 4, where the differences were over 100 MPa after the start of mould filling. In contrast, at point 5, the compressive stresses were lower, in the lower tens of MPa for variant D.
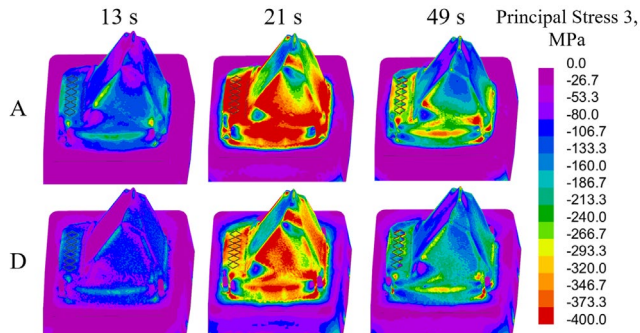

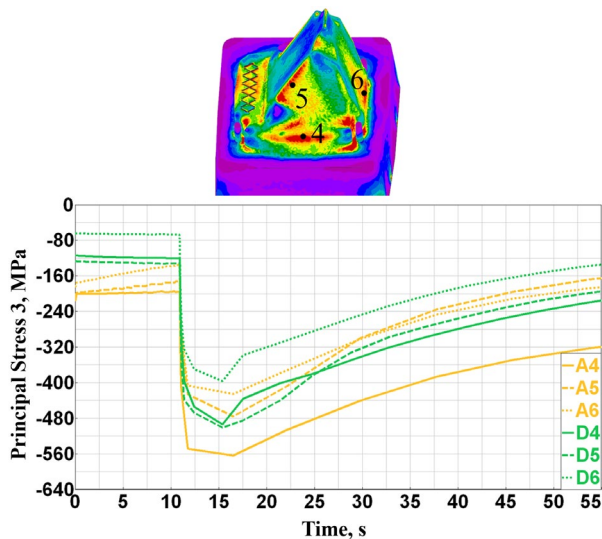Fig. 8. Principal Stress 3 in insert variants A and D

Fig. 9. Profiles of Principal Stress 3 at selected insert points

Figure 10 shows Principal Stress 1 on the insert sections of variants A and D at different stages of the cycle. This result shows the areas most stressed by tensile stress, applied predominantly in the insert volume. The occurrence of tensile stresses was again related to the temperature regime of the mould. The highest tensile stresses were observed between 13 and 21 seconds in the cycle, during filling and solidification of the casting. During this period, the largest temperature differences occurred in the inserts between the outer layers of the material and the cooled volume of the insert. The areas of material around the cooling channels tended to shrink due to the lower temperature, causing tensile stresses to develop. Variant A had higher tensile stresses throughout the cycle compared to variant D. This effect was due to the timing of the cooling. Variant A was cooled with a constant water flow throughout the cycle (see Table 2), i.e. even in the phases when the insert was not in contact with the hot metal. After removal of the casting, the insert was not completely cooled to ambient temperature and, therefore, the effect of the cooling

channel in the vicinity of which the insert temperatures reached lower values can be seen here as well. This resulted in tensile stresses around the cooling channel. In this respect, the stress state of variant D was more favourable. It should be noted that no stresses exceeding the yield strength of the material were found in the inserts tested. At the same time, the risk of plastic deformation fatigue was not predicted in the inserts examined.
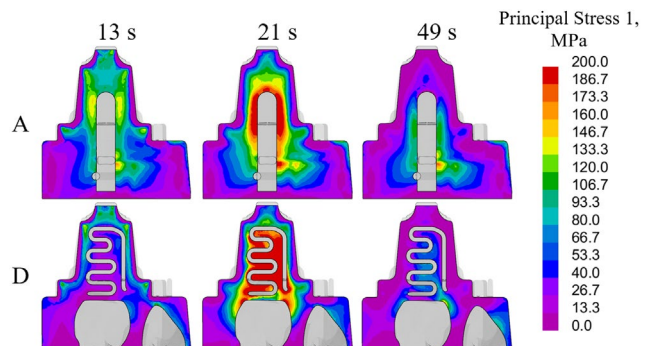

Fig. 10. Principal Stress 1 on insert sections of variants A and D

Figure 11 shows the tensile stress profile in the tip of the insert of variants A and D. The tensile stress profile in the tip of the insert is almost unchanged due to the conformal cooling. Stresses in this region were found to reach a maximum of 160 MPa for variant A and 150 MPa for variant D. These values are well below the yield strength of the material at the given temperatures.

Figure 12 compares the Fatigue life indicator, which provides a qualitative estimate of the core life of variants A and D. As the previous results show, the working part of the insert in contact with the metal was subjected to the highest stress during the cycle. This area is also where the greatest risk of exceeding fatigue strength exists for both variants. Based on the results in Figure 12, the insert of variant D with conformal cooling has the potential for higher durability.

Figure 13 shows the results of Contact Pressure, which is generated between the insert, the casting and the adjacent parts of the mould due to deformation of the individual components. The Contact Pressure between the mould components can cause wear due to friction when opening the mould. In the case of a casting, surface damage may occur during removal from the mould. As can be seen in Figure 13, in the case of the insert under evaluation, the contact pressure was mainly between the insert and the casting, with a more extensive area of action for variant A. For variant D, the area of contact pressure between the insert and the other components was significantly reduced.
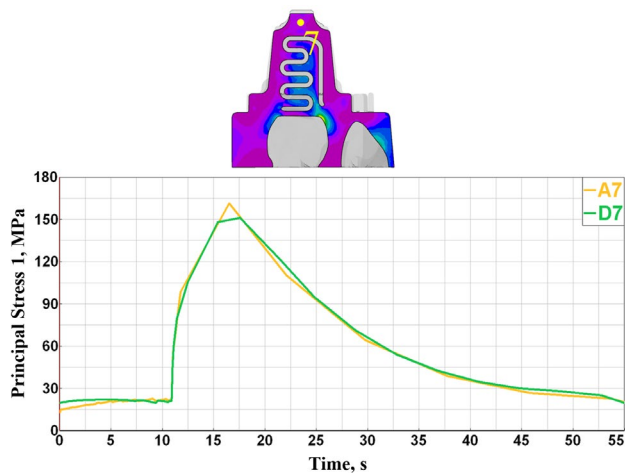
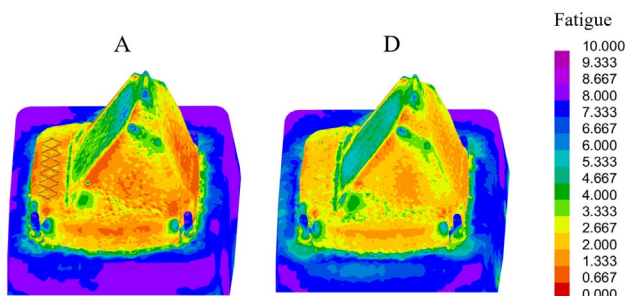Fig. 11. Profile of Principal Stress 1 in the tip of the insert

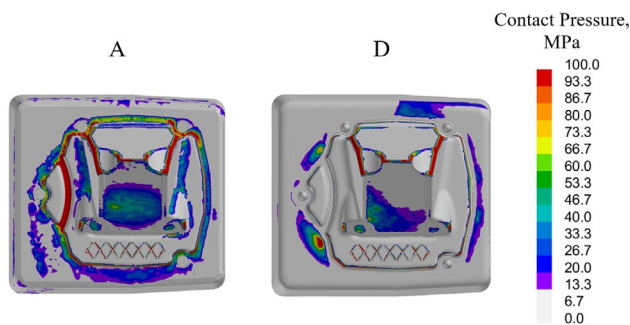Fig. 12. Comparison of fatigue life of inserts of variants A and D

Fig. 13. Comparison of Contact Pressure of variants A and D

5.3. Casting quality

Numerical simulations of mould filling and solidification of the casting were carried out to map the effect of the conformal cooling of the insert on the casting quality. The mould filling was not affected by the change in cooling, so these results will not be presented here.

Figure 14 shows the results of the porosity prediction in the castings from variants A and D. The cooling modification had a minimal effect on the occurrence of porosity. The position of the areas likely to have porosity did not change. There was a change in the size of some areas of porosity, but to an extent that is

negligible in the context of realistic operating conditions. In terms of porosity, it can be said that the quality of the casting was maintained after the change in cooling.
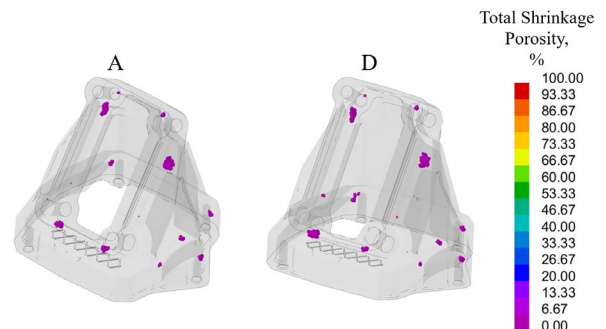

Fig. 14. Prediction of porosity in variant A and D castings (Cut Off > 5 %)

Figure 15 shows the tensile stress results in the castings of variants A and D before and after removal from the mould. Before removal, higher tensile stresses existed in the castings of both variants, which exceeded the material strength limit (240 MPa [25]) in some places. This was due to the castings remaining in the mould, which inhibited their deformation. After removal, most of the tensile stresses were relaxed and the casting reached a more favourable stress state. However, there were still places in the castings that, according to the simulation, could be risky and the yield strength of the material (140 MPa [25]) could be exceeded. When comparing the castings of variants A and D, there were no significant changes in the stress ratios in the castings. It can be said that after the application of conformal cooling, there was a slight decrease in the tensile stresses in the casting of variant D, but this decrease would probably not be reflected in real conditions.
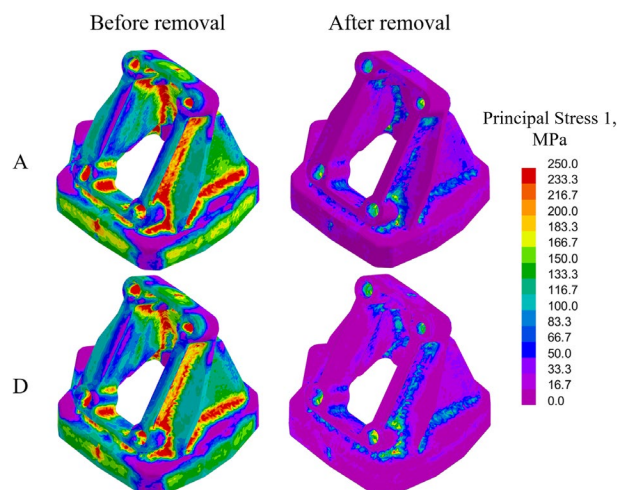

Fig. 15. Principal Stress 1 in casting variants A and D

Due to the presence of higher tensile stresses in the castings, the Hot Tearing Indicator criterion, which predicts the susceptibility of castings to hot cracking, was further analysed. The results of the Hot Tearing Indicator are presented in

Figure 16. Low values of the criterion were calculated in the castings of both variants, indicating a low risk of cracking in the castings. This also corresponds to the state of production under operating conditions. In the case of the studied casting, no quality reduction due to the presence of cracks has been observed so far.
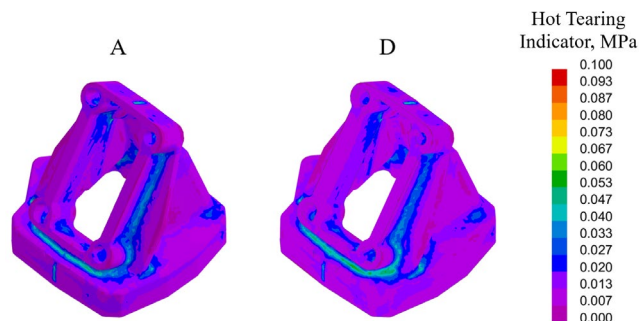

Fig. 16. Hot Tearing Indicator in variant A and D castings

6. Conclusions

This paper dealt with the design of conformal cooling of an insert, which is part of a mould for High-Pressure Die Casting of aluminium alloys. Numerical simulations were performed in ProCAST software to verify the cooling effect. A total of 4 variants were simulated, of which variant A contained the current cooling channel geometry and the remaining 3 variants contained different designs for the conformal cooling design. For the variants with conformal cooling, the insert was also lightened to save material for manufacturing. The numerical simulations were divided into two phases. In the first phase, cycling was simulated focusing on the mould temperature field. Based on these results, the design with the most suitable conformal cooling execution was selected, for which mould filling and solidification of the casting, including stress states, were further simulated. Attention was also paid to the quality parameters of the casting. The findings can be summarised in the following points:

- Based on the results of the temperature field during cycling, variant D of the insert with conformal cooling was selected for further analysis. This variant had a good cooling effect on the working parts of the insert even when the cooling interval was reduced. There was an overall temperature increase in the base of the insert due to material loss during lightening. However, this did not have a negative effect, as confirmed by further analysis.
- During the cycle, the insert was most stressed by compressive stress exceeding 400 MPa, caused by the heating of the surface layers of the working part of the insert and expansion of the material. The compressive stress load on the working part of the insert was reduced with the application of the conformal cooling variant D.
- The tensile stress, caused by the shrinkage of the material as the temperature dropped, acted mainly in the vicinity of the cooling channels. In the phase of the highest thermal loading on the insert (between 11 and 21 seconds of the cycle), the tensile stresses of variants A and D were at a similar level. For the remainder of the cycle, the tensile

stresses were higher for variant A, which was cooled throughout the cycle. Thus, by adjusting the cooling interval, the tensile stress loading was partially reduced for variant D.
- In variant D, the Contact Pressure area between the insert, casting, and adjacent mould components was reduced. This means that there is a lower risk of frictional wear of the mould components and damage to the casting surface.
- No negative impacts of the change in the cooling of the insert on the quality of the casting were found. The predicted areas of porosity hardly changed. There were also no significant changes in the stress states. Stress-induced defects were not predicted for this type of casting.
- Variant D also had the advantage of lightening, saving 7.2 kg of material per insert produced, which makes up 28% of the original weight of the insert.

Based on the results, variant D of the insert with conformal cooling was recommended for production by 3D printing. After heat treatment, machining, and coating, it will be subjected to durability testing under MOTOR JIKOV operating conditions in the following phase of the research.

Acknowledgements

References

[1] Feng, S., Kamat, A.M. & Pei, Y. (2021). Design and fabrication of conformal cooling channels in molds: Review and progress updates. *International Journal of Heat and Mass Transfer*. 171, 121082, 1-28. DOI: 10.1016/j.ijheatmasstransfer.2021.121082

[2] Klobčar, D., Tušek, J. & Taljat, B. (2008). Thermal fatigue of materials for die-casting tooling. *Materials Science and Engineering: A*. 472 (1-2), 198-207. DOI: 10.1016/j.msea.2007.03.025.

[3] Anand, A., Nagarajan, D., El Mansori, M. & Sivarupan, T. (2023). Integration of additive fabrication with high-pressure die casting for quality structural castings of aluminium alloys; optimising energy consumption. *Transactions of the Indian Institute of Metals*. 76(2), 347-379. DOI: 10.1007/s12666-022-02750-y.

[4] Chen, G., Wang, J., Wang, D., Xue, L., Zeng, B. & Qin, B. (2021). Effect of liquid oxy-nitriding at various temperatures on wear and molten aluminum corrosion behaviors of AISI H13 steel. *Corrosion Science*. 178, 109088. DOI: 10.1016/j.corsci.2020.109088.

[5] Bhaskar, M., Anand, G., Nalluswamy, T. & Suresh, P. (2022). Die life in aluminium high-pressure die casting

industries. *Journal of The Institution of Engineers (India): Series D*. 103(1), 117-123. DOI: 10.1007/s40033-021-00317-7.

[6] Andronov, V., Beránek, L., Zajíc, J., Šotka, P. & Bock, M. (2023). Case study of large three-dimensional-printed slider with conformal cooling for high-pressure die casting. *3D Printing and Additive Manufacturing*. 10(4), 587-608. DOI: 10.1089/3dp.2022.0225.

[7] Jarfors, A.E.W., Sevastopol, R., Seshendra, K., Zhang, Q., Steggo, J. & Stolt, R. (2021). On the use of conformal cooling in high-pressure die-casting and semisolid casting. *Technologies*. 9(2), 39, 1-16. DOI: 10.3390/technologies9020039.

[8] Fiorentini, F., Curcio, P., Armentani, E., Rosso, C. & Baldissera, P. (2019). Study of two alternative cooling systems of a mold insert used in die casting process of light alloy components. *Procedia Structural Integrity*. 24, 569-582. DOI: 10.1016/j.prostr.2020.02.050.

[9] Stolt, R., Pour, M.A. & Siafakas, D. (2021). Making additively manufactured cores with conformal tooling directly on a die-base. *Procedia Manufacturing*. 55, 200-204. https://doi.org/10.1016/j.promfg.2021.10.028.

[10] Barreiro, P., Armutcu, G., Pfrimmer, S. & Hermes, J. (2022). Quality improvement of an aluminum gearbox housing by implementing additive manufacturing. *Forschung im Ingenieurwesen*. 86(3), 605-616. DOI: 10.1007/s10010-021-00541-3.

[11] Shinde, M.S. & Ashtankar, K.M. (2017). Additive manufacturing–assisted conformal cooling channels in mold manufacturing processes. *Advances in Mechanical Engineering*. 9(5), 1-14. DOI: 10.1177/1687814017699764.

[12] Armillotta, A., Baraggi, R. & Fasoli, S. (2014). SLM tooling for die casting with conformal cooling channels. *The International Journal of Advanced Manufacturing Technology*. 71(1-4), 573-583. DOI: 10.1007/s00170-013-5523-7.

[13] Zeng, T., Abo-Serie, E., Henry, M. & Jewkes, J. (2023). Cooling channel free surface optimisation for additively manufactured casting tools. *The International Journal of Advanced Manufacturing Technology*. 127(3-4), 1293-1315. DOI: 10.1007/s00170-023-11402-4.

[14] Karakoc, C., Dizdar, K. C. & Dispinar, D. (2022). Investigation of effect of conformal cooling inserts in high-pressure die casting of AlSi9Cu3. *The International Journal of Advanced Manufacturing Technology*. 121(11-12), 7311-7323. DOI: 10.1007/s00170-022-09808-7.

[15] Anglada, E., Meléndez, A., Vicario, I., Arratibel, E. & Aguillo, I. (2015). Adjustment of a high pressure die casting simulation model against experimental data. *Procedia Engineering*. 135, 966-973. DOI: 10.1016/j.proeng.2015.12.584.

[16] Norwood, A., Dickens, P., Soar, R., Harris, R., Gibbons, G. & Hansell, R. (2004). Analysis of cooling channels performance. *International Journal of Computer Integrated Manufacturing*. 17(8), 669-678. DOI: 10.1080/0951192042000237528.

[17] Piekło, J., Burbelko, A. & Garbacz-Klempka, A. (2022). Shape-dependent strength of Al Si9Cu3FeZn die-cast alloy in impact zone of conformal cooling core. *Materials*. 15(15), 5133, 1-21. DOI: 10.3390/ma15155133.

[18] ESI Group. (2024, April). *ProCAST*. Retrieved April 05, 2024, from https://www.esi-group.com/products/procast.

[19] ESI Group. (2021, August). *ProCAST 2021.0 – User Guide*. Retrieved April 05, 2024, from https://myesi.esi-group.com/downloads/software-documentation/procast-2021.0-user-guide-visual-cast-procast-rev-b-online-online-online-online.

[20] Ingham, D.B., Ma, L. (2005). Fundamental equations for CFD in river flow simulations. In P.D. Bates, S.N. Lane, R.I. Ferguson (Eds.), *Computational Fluid Dynamics: Applications in Environmental Hydraulics* (pp. 19-50). New Jersey: Wiley.

[21] Alhendal, Y., Turan, A. (2012). Volume-of-fluid (VOF). In R. Petrova (Eds.), *Finite Volume Method - Powerful Means of Engineering Designs* (pp. 215-234). Rijeka: InTech.

[22] Yeoh, G.H., Tu, J. (2019). *Computational Techniques for Multiphase Flows*. Cambridge: Elsevier. Butterworth-Heinemann.

[23] Ranade, V.V. (2002) *Computational Flow Modeling for Chemical Reactor Engineering*. Cambridge: Elsevier.

[24] Colosio. (2022, October). *PFO Series*. Retrieved September 6th, 2024, from https://www.colosiopresse.it/docs/PFO_Colosio_Datasheet_EN.pdf

[25] Uddeholm. (2018, May). *Uddeholm Dievar*. Retrieved September 3rd, 2024, from https://www.uddeholm.com/app/uploads/sites/216/productdb/api/tech_uddeholm-dievar_en.pdf

[26] ČSN EN 1706+A1. (2022). *Aluminium and aluminium alloys – Castings – Chemical composition and mechanical properties*. Prague: Czech Standardization Agency.